ACS MEASUREMENT SCIENCE Au
AN OPEN ACCESS JOURNAL OF THE AMERICAN CHEMICAL SOCIETY

pubs.acs.org/measureau

Letter

Artificial Synapse: Spatiotemporal Heterogeneities in Dopamine Electrochemistry at a Carbon Fiber Ultramicroelectrode

Baoping Chen, David Perry, James Teahan, Ian J. McPherson, James Edmondson, Minkyung Kang, Dimitrios Valavanis, Bruno G. Frenguelli, and Patrick R. Unwin*

Cite This: *ACS Meas. Au* 2021, 1, 6–10

Read Online

ACCESS | Metrics & More | Article Recommendations | Supporting Information

ABSTRACT: An artificial synapse is developed that mimics ultramicroelectrode (UME) amperometric detection of single cell exocytosis. It comprises the nanopipette of a scanning ion conductance microscope (SICM), which delivers rapid pulses of neurotransmitter (dopamine) locally and on demand at >1000 defined locations of a carbon fiber (CF) UME in each experiment. Analysis of the resulting UME current-space-time data reveals spatiotemporal heterogeneous electrode activity on the nanoscale and submillisecond time scale for dopamine electrooxidation at typical UME detection potentials. Through complementary surface charge mapping and finite element method (FEM) simulations, these previously unseen variations in electrochemical activity are related to heterogeneities in the surface chemistry of the CF UME.

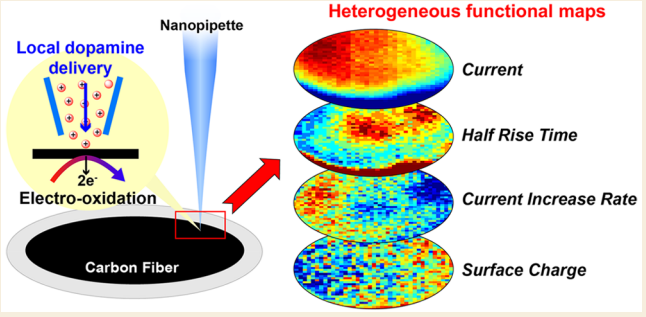

KEYWORDS: *Scanning Ion Conductance Microscopy (SICM), Electrochemical Imaging, Exocytosis, Nanopipettes, Single Entity Electrochemistry*

Synaptic signal transmission is the primary mechanism of cell to cell communication in the nervous system, for which vesicular exocytosis from an emitting cell is a key process.[1] Exocytosis involves (part) fusion of a vesicle with the inside of the emitting cell membrane to create a fusion pore from which the vesicle contents are released.[2,3] Mechanistic aspects of vesicular release have been studied by using a carbon fiber (CF) ultramicroelectrode (UME), positioned close to a target single cell, to monitor exocytotic events upon cell stimulation[4−8] via chronoamperometric (current−time) detection of electroactive neurotransmitters via electrooxidation. This configuration results in highly localized transient electrochemical detection at the UME because the vesicular sources are tens to hundreds of nanometers in diameter, with the size depending on the neuron type.[7] Herein, we introduce a scanning ion conductance microscopy (SICM) system that enables the delivery of rapid pulses of dopamine transiently and locally, at thousands of defined locations at a CF UME, mimicking exocytosis cell release-UME detection. The electrochemical signatures are analyzed and related to the nanoscale electrode surface properties *at the locations where the responses are measured*. This allows us to determine whether local electrode surface properties have any bearing on the chronoamperometric response at a CF UME.

SICM is a noncontact scanning probe microscopy technique that employs a nanopipette tip, enabling multifunctional mapping of a wide range of surface properties.[9−12] For this work, we used single-barrel nanopipette tips (~100 nm diameter; SI, Figure S1), filled with an aqueous solution of 100 mM dopamine hydrochloride (pH 5.8) of the same order of concentration as in a vesicle,[13,14] whose contents could be released and collected on demand at a CF UME (~7 μm diameter) surface. This configuration creates an artificial synapse[15] that mimics the time scale and spatial dimension of a single cell synaptic release measurement (Figures 1 and Figure S2). HEPES physiological saline, containing 150 mM NaCl and 10 mM HEPES (pH 7.4), was used as the (bulk) electrolyte, which bathed the CF UME. Two Ag/AgCl electrodes were used as quasi-reference counter electrodes (QRCEs), one in the bulk solution ($QRCE_{bulk}$), and the other inside the tip ($QRCE_{tip}$). With the CF UME (working electrode) at ground, adjustment of the $QRCE_{bulk}$ potential versus ground served to control the CF UME potential with respect to $QRCE_{bulk}$. Further details on the experiments, including equilibrium potentials of the two QRCEs and the electrochemical setup, are provided in SI-1 and SI-2.

Electrode mapping utilized a hopping-potential pulse mode of SICM, with the protocol for a single pixel illustrated in Figure 1.

Received: May 6, 2021
Published: July 1, 2021

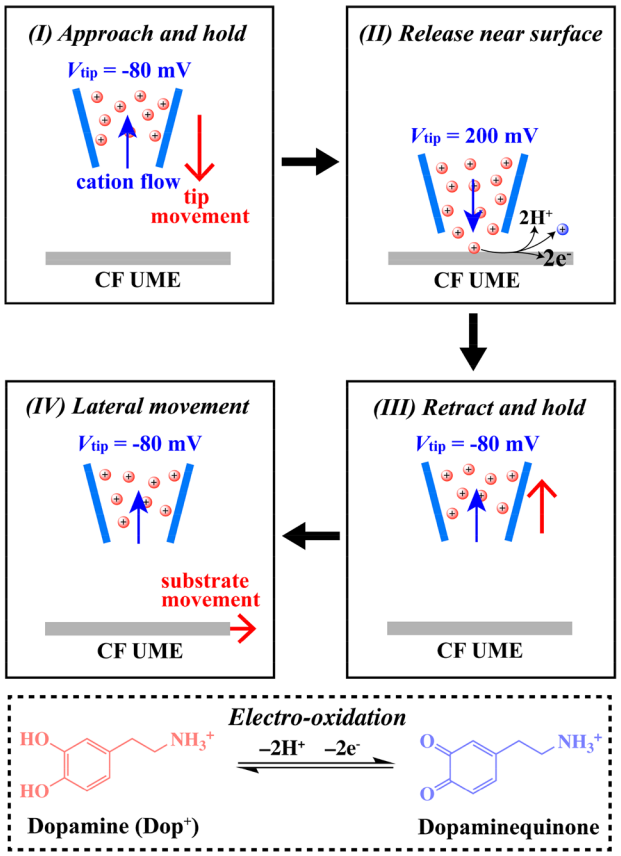

Figure 1. Schematic of the main features of the SICM hopping-potential pulse protocol, illustrating the translation of the tip and changes in the applied potential to enable the controlled release of Dop^+ at a single pixel (described in the text). The procedure was repeated >1000 times in fresh locations across a predefined grid over the UME. The inset schematic illustrates the major dopamine electrooxidation process.

(I) The tip was translated toward the UME substrate with $QRCE_{tip}$ biased at −80 mV with respect to $QRCE_{bulk}$ to produce an ionic current that was sensitive to the vertical position of the tip near the UME surface,[16] while holding the protonated dopamine (Dop^+) in the tip.[17] At this small potential bias, the SICM response is primarily sensitive to tip−substrate distance.[18] (II) When the tip reached the near surface, Dop^+ was released by stepping V_{tip} to 200 mV versus $QRCE_{bulk}$ for 20 ms. (III) Dop^+ release was terminated by stepping V_{tip} back to −80 mV, as the tip was simultaneously retracted to the bulk. (IV) After 200 ms to allow re-establishment of initial conditions,[19] the UME was moved laterally and the same procedure was executed at the next (fresh) point on the surface. The UME was biased at 0.7 V throughout (relative to $QRCE_{bulk}$), at the diffusion-limit for electrooxidation of Dop^+ as determined by voltammetry at the entire UME (see SI-3), and typical of that applied in amperometric monitoring of exocytosis.[7,8] Both the tip and substrate currents were measured continuously throughout.

For SICM mapping, the tip (~100 nm diameter) was approached to a working distance of ~37 nm, as estimated from finite element method (FEM) simulations (see SI-6), for a decrease in the tip current magnitude by 2% from the bulk value at each approach. We are interested in situations where the nanopipette tip is directly over the CF surface to mimic the detection of exocytotic release, and exemplar data cropped to the central ~6 μm diameter of the CF (to avoid complications from edge effects) are shown in Figure 2 in several different forms. Figure 2a shows 3 example substrate current−time (I_{sub}-t) transients, at different locations of the CF UME (marked in Figure 2b). The I_{sub}-t curves have the same general shape, that is, I_{sub} rises to a quasi-steady value after a short delay, but there are differences in the magnitude of I_{sub}.

The extent to which the current response is heterogeneous across the UME substrate is evident from Figure 2b, which shows a map of the final I_{sub} for each pulse release; the current varies by ~33% (minimum to maximum value). Figure 2c further highlights heterogeneous activity in the time dimension,

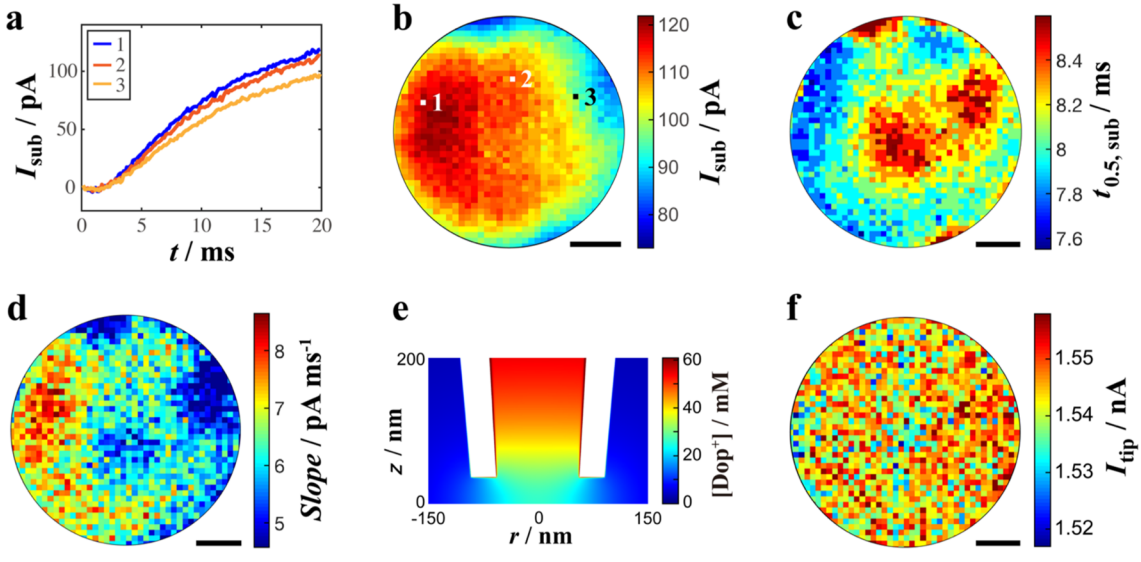

Figure 2. (a) Three typical I_{sub}-t transients at pixels marked in (b). Images across the central 6 μm diameter of a CF UME of (b) final value of I_{sub} for each release pulse, (c) time for I_{sub} to reach half the final value, (d) rate of increase of I_{sub} at a time of 2.5 ms after the pulse, and (f) I_{tip} at the end of potential pulse. (e) Typical simulated concentration profile for Dop^+ at the end of pulse release, with a rate of electrooxidation commensurate with the experimentally observed UME current values, in this case a current of 88 pA at the end of the Dop^+ release pulse (see SI, Figure S12). Step size between pixels: 150 nm, with no interpolation of data. Scale bar: 1.2 μm.

https://doi.org/10.1021/acsmeasuresciau.1c00006
ACS Meas. Au 2021, 1, 6−10

showing sub-millisecond variations in the time for I_{sub} to reach half the final value, while Figure 2d maps the rate of increase of I_{sub} at a time of 2.5 ms after the Dop^+ pulse, again highlighting spatiotemporal variations in electrode activity. The spatial resolution is time-dependent, as evident from Movie S1 (see SI-8, cf., 4 ms where strongly localized activity is evident with 10 ms where there is still heterogeneous activity, but a radial component due to Dop^+ lateral diffusion emerges in the background current). This is also seen when comparing Figure 2d (at 2.5 ms) with Figure 2b (at 20 ms), albeit for different activity signatures. This is consistent with the simulated concentration profile for Dop^+ undergoing oxidation at the UME surface at a typical current of 88 pA (Figure S12). While the Dop^+ detection potential of the CF UME was set to mimic exocytosis-UME detection protocols[7,8,20] and is in the diffusion-limited region based on the bulk voltammogram for 1 mM Dop^+ in SI (Figure S4), the reaction is not diffusion-limited for nanoscale delivery-detection; the near interface concentration of Dop^+ is finite, ~20 mM in the region of the CF UME directly under the center of the nanopipette. Kinetic limitations are manifest as a significant anodic shift of Dop^+ electrooxidation potential for adsorbed Dop^+ at short time scales,[21] and an anodic shift of the electrooxidation potential under exocytosis-UME detection measurements might further be expected due to the high Dop^+ concentration oxidized locally and the consequent high local concentration of protons released (given the comparatively low buffer concentration herein and in typical exocytosis-UME measurements).[2−4,6,8,15]

To further highlight the reliability of these measurements, the I_{sub}-t profile measured in our experiments is reproduced well in simulations, with a simple electrooxidation rate boundary condition (Dop^+ flux) as the only adjustable parameter, as detailed in SI-7, and taking account of the RC time constant of the CF UME-artificial synapse.[22,23] Importantly, the tip current (I_{tip}) at the end of the pulse potential period is consistent at each pixel, varying by just a few percent from minimum to maximum across ~1200 positions at all times (Figure 2f, Movie S2). This confirms the stability and consistency of the SICM delivery process, which is also evidenced by the narrow distribution of half time (1.25 ± 0.03 ms) for the tip release process in Figure S3c, defined as the time for I_{tip} to attain 50% of the final magnitude change. These results prove that the observed variations in the electrochemical response of the CF UME are due to heterogeneous electrode activity. Typical tip and substrate current−time behavior and substrate topography over the UME and surrounding glass are shown in Figure S3.

We now consider the origin of the heterogeneities in spatiotemporal electrochemical activity at the CF UME. Correlative electrochemical imaging−Raman microscopy has recently been used to analyze variations in dopamine electrooxidation at screen printed carbon electrodes,[24] but the spatial variations in electrochemical activity observed in Figure 2 are beyond the diffraction limit. A qualitative indicator of variations in surface chemistry of the CF UME can be seen from contrast variations in field emission-scanning electron microscopy (FE-SEM) images of a typical CF UME surface (Figure S5); there is less charging (darker contrast) for more conductive regions and vice versa.[25] These spatial heterogeneities occur on the several hundred nanometer scale, similar to the spatial variations in CF UME current for Dop^+ electrooxidation.

To understand how electrode surface chemistry could influence the Dop^+ electrooxidation current signal, we used SICM to map the surface charge of the CF UME (see SI-5),[18] and the result was compared directly with the corresponding co-located electrochemical activity. Surface charge data were obtained in a separate scan just before the electrochemical activity mapping. The coalignment of electrode activity and surface charge maps is detailed in Figure S7. A surface charge map of the CF UME surface in the region of interest (extracted from the data in Figure S7), at a CF UME bias of V_{sub} = 0.7 V, as used for activity mapping, is shown in Figure 3a. There are

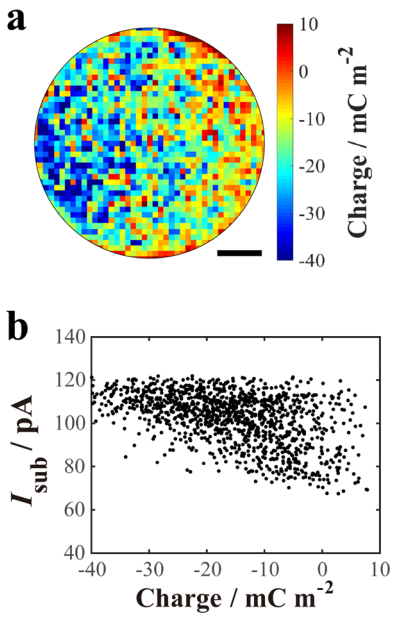

Figure 3. (a) Image of quantified surface charge in the same area of the CF UME as the electrochemical maps in Figure 2. Scale bar: 1.2 μm. (b) Correlation between I_{sub} and local surface charge at the CF UME surface.

significant surface charge heterogeneities across the CF surface. There is predominantly a negative surface charge density at the carbon electrode surface,[26] attributed to the prevalence of surface oxygen-containing moieties on carbon electrodes, for example, surface oxides[27] and surface carboxylates.[28−30] Dop^+ is considered to adsorb to these groups,[31] and, even without adsorption, would be a significant component of the charge-compensating double layer under the experimental conditions. At least in part, the higher concentrations of Dop^+ in these locations and the fact that adsorbed Dop^+ may catalyze the oxidation of solution-phase Dop^+[32] explains the plot of I_{sub} versus CF UME local surface charge density in Figure 3b, where higher electrochemical currents are generally obtained in regions with more negative electrode surface charge. Surface roughness at the nanoscale and the nature of the resulting surface sites exposed[33] will also be important for Dop^+ electrooxidation kinetics, and Dop^+ adsorption.[21]

In conclusion, this study reveals spatiotemporal variations in the rate of dopamine electrooxidation across a CF UME surface under conditions that mimic the amperometric detection of single cell exocytosis. Analysis of single cell exocytosis often involves the measurement of peak rise time (related to the opening kinetics of the fusion pore) and the peak (spike) half-width, which is indicative of the length of the duration event.[7] Figure 2c is a proxy for such measurements, and the overall variation between different electrode locations is on the sub-millisecond time scale (Figure 2). This is significant because exocytosis measurements usually report 1 ms (or longer) time

https://doi.org/10.1021/acsmeasuresciau.1c00006
ACS Meas. Au 2021, 1, 6−10

resolution.[34,35] Heterogeneity in activity becomes a more important consideration for faster measurements, where detection is more localized (less lateral diffusion to neighboring sites on the electrode), although there maybe scope for using higher oxidation potentials to push detection closer to the diffusion limit, being mindful of the onset of the anodic oxidation of water and the CF UME.

■ ASSOCIATED CONTENT

Supporting Information

The Supporting Information is available free of charge at https://pubs.acs.org/doi/10.1021/acsmeasuresciau.1c00006.

Typical STEM image of the nanopipettes used in this work, details about the experiments, voltammetric and FE-SEM characterizations of a typical CF UME, data of the tip and substrate current−time behavior over the UME and surrounding glass, as well as the maps of substrate topography and surface charge, and FEM model details and simulations for the investigation of time response of the electrochemical cell (PDF)

Movie of I_{sub}-t during the pulse delivery (AVI)

Movie of I_{tip}-t during the pulse delivery (AVI)

■ AUTHOR INFORMATION

Corresponding Author

Patrick R. Unwin − *Department of Chemistry, University of Warwick, Coventry CV4 7AL, United Kingdom;* orcid.org/0000-0003-3106-2178; Email: p.r.unwin@warwick.ac.uk

Authors

Baoping Chen − *Department of Chemistry, University of Warwick, Coventry CV4 7AL, United Kingdom;* orcid.org/0000-0002-5944-092X

David Perry − *Department of Chemistry, University of Warwick, Coventry CV4 7AL, United Kingdom;* orcid.org/0000-0002-8630-4798

James Teahan − *Department of Chemistry and Molecular Analytical Science Centre for Doctoral Training, University of Warwick, Coventry CV4 7AL, United Kingdom*

Ian J. McPherson − *Department of Chemistry, University of Warwick, Coventry CV4 7AL, United Kingdom;* orcid.org/0000-0002-9377-515X

James Edmondson − *Department of Chemistry and Molecular Analytical Science Centre for Doctoral Training, University of Warwick, Coventry CV4 7AL, United Kingdom*

Minkyung Kang − *Department of Chemistry, University of Warwick, Coventry CV4 7AL, United Kingdom;* orcid.org/0000-0003-3248-8496

Dimitrios Valavanis − *Department of Chemistry, University of Warwick, Coventry CV4 7AL, United Kingdom;* orcid.org/0000-0002-8777-664X

Bruno G. Frenguelli − *School of Life Sciences, University of Warwick, Coventry CV4 7AL, United Kingdom*

Complete contact information is available at: https://pubs.acs.org/10.1021/acsmeasuresciau.1c00006

Notes

The authors declare no competing financial interest.

■ ACKNOWLEDGMENTS

B.C. was supported by the Warwick−China Scholarship Council for a joint scholarship. D.P. was supported by a Leverhulme Trust Research Project Grant. J.T. and J.E. thank the EPSRC for PhD studentships through the EPSRC Center for Doctoral Training in Molecular Analytical Science (grant EP/L015307/1). I.J.M. and P.R.U. acknowledge an EPSRC Program Grant (grant EP/R018820/1). D.V. and P.R.U. acknowledge support from the European Union's Horizon 2020 research and innovation programme under Marie Skłodowska-Curie MSCA-ITN Single-Entity Nanoelectrochemistry, SENTINEL [812398]. P.R.U. thanks the Royal Society for a Wolfson Research Merit Award.

■ REFERENCES

(1) Burgoyne, R. D.; Morgan, A. Secretory Granule Exocytosis. *Physiol. Rev.* **2003**, *83* (2), 581−632.

(2) Wightman, R. M.; Haynes, C. L. Synaptic Vesicles Really Do Kiss and Run. *Nat. Neurosci.* **2004**, *7* (4), 321−322.

(3) Oleinick, A.; Svir, I.; Amatore, C. 'Full Fusion'Is Not Ineluctable during Vesicular Exocytosis of Neurotransmitters by Endocrine Cells. *Proc. R. Soc. London, Ser. A* **2017**, *473* (2197), 20160684.

(4) Wightman, R.; Jankowski, J.; Kennedy, R.; Kawagoe, K.; Schroeder, T.; Leszczyszyn, D.; Near, J.; Diliberto, E.; Viveros, O. Temporally Resolved Catecholamine Spikes Correspond to Single Vesicle Release from Individual Chromaffin Cells. *Proc. Natl. Acad. Sci. U. S. A.* **1991**, *88* (23), 10754−10758.

(5) Wightman, R. M. Probing Cellular Chemistry in Biological Systems with Microelectrodes. *Science* **2006**, *311* (5767), 1570−1574.

(6) Amatore, C.; Arbault, S.; Guille, M.; Lemaitre, F. Electrochemical Monitoring of Single Cell Secretion: Vesicular Exocytosis and Oxidative Stress. *Chem. Rev.* **2008**, *108* (7), 2585−2621.

(7) Phan, N. T.; Li, X.; Ewing, A. G. Measuring Synaptic Vesicles Using Cellular Electrochemistry and Nanoscale Molecular Imaging. *Nature Rev. Chem.* **2017**, *1* (6), 0048.

(8) Li, X.; Dunevall, J.; Ewing, A. G. Using Single-Cell Amperometry To Reveal How Cisplatin Treatment Modulates the Release of Catecholamine Transmitters during Exocytosis. *Angew. Chem., Int. Ed.* **2016**, *55*, 9041−9044.

(9) Zhu, C.; Huang, K.; Siepser, N. P.; Baker, L. A. Scanning Ion Conductance Microscopy. *Chem. Rev.* **2020**, DOI: 10.1021/acs.chemrev.0c00962.

(10) Perry, D.; Paulose Nadappuram, B.; Momotenko, D.; Voyias, P. D.; Page, A.; Tripathi, G.; Frenguelli, B. G.; Unwin, P. R. Surface Charge Visualization at Viable Living Cells. *J. Am. Chem. Soc.* **2016**, *138* (9), 3152−3160.

(11) Zhou, L.; Gong, Y.; Sunq, A.; Hou, J.; Baker, L. A. Capturing Rare Conductance in Epithelia with Potentiometric-Scanning Ion Conductance Microscopy. *Anal. Chem.* **2016**, *88* (19), 9630−9637.

(12) Zhou, L.; Gong, Y.; Hou, J.; Baker, L. A. Quantitative Visualization of Nanoscale Ion Transport. *Anal. Chem.* **2017**, *89* (24), 13603−13609.

(13) Dunevall, J.; Fathali, H.; Najafinobar, N.; Lovric, J.; Wigström, J.; Cans, A.-S.; Ewing, A. G. Characterizing the Catecholamine Content of Single Mammalian Vesicles by Collision-Adsorption Events at an Electrode. *J. Am. Chem. Soc.* **2015**, *137* (13), 4344−4346.

(14) Colliver, T.; Pyott, S.; Achalabun, M.; Ewing, A. G. VMAT-Mediated Changes in Quantal Size and Vesicular Volume. *J. Neurosci.* **2000**, *20* (14), 5276−5282.

(15) Cans, A.-S.; Wittenberg, N.; Eves, D.; Karlsson, R.; Karlsson, A.; Orwar, O.; Ewing, A. Amperometric Detection of Exocytosis in an Artificial Synapse. *Anal. Chem.* **2003**, *75* (16), 4168−4175.

(16) Chen, C.-C.; Zhou, Y.; Baker, L. A. Scanning Ion Conductance Microscopy. *Annu. Rev. Anal. Chem.* **2012**, *5*, 207−228.

(17) Chen, B.; Perry, D.; Page, A.; Kang, M.; Unwin, P. R. Scanning Ion Conductance Microscopy: Quantitative Nanopipette Delivery-

Substrate Electrode Collection Measurements and Mapping. *Anal. Chem.* **2019**, *91* (3), 2516−2524.
(18) Page, A.; Perry, D.; Young, P.; Mitchell, D.; Frenguelli, B. G.; Unwin, P. R. Fast Nanoscale Surface Charge Mapping with Pulsed-Potential Scanning Ion Conductance Microscopy. *Anal. Chem.* **2016**, *88* (22), 10854−10859.
(19) Momotenko, D.; Girault, H. H. Scan-Rate-Dependent Ion Current Rectification and Rectification Inversion in Charged Conical Nanopores. *J. Am. Chem. Soc.* **2011**, *133* (37), 14496−14499.
(20) Trouillon, R.; Ewing, A. G. Single Cell Amperometry Reveals Glycocalyx Hinders the Release of Neurotransmitters during Exocytosis. *Anal. Chem.* **2013**, *85* (9), 4822−4828.
(21) Oleinick, A.; Álvarez-Martos, I.; Svir, I.; Ferapontova, E. E.; Amatore, C. Surface Heterogeneities Matter in Fast Scan Cyclic Voltammetry Investigations of Catecholamines in Brain with Carbon Microelectrodes of High-Aspect Ratio: Dopamine Oxidation at Conical Carbon Microelectrodes. *J. Electrochem. Soc.* **2018**, *165* (12), G3057.
(22) Chen, C.-H.; Ravenhill, E. R.; Momotenko, D.; Kim, Y.-R.; Lai, S. C. S.; Unwin, P. R. Impact of Surface Chemistry on Nanoparticle-Electrode Interactions in the Electrochemical Detection of Nanoparticle Collisions. *Langmuir* **2015**, *31* (43), 11932−11942.
(23) Robinson, D. A.; Edwards, M. A.; Ren, H.; White, H. S. Effects of Instrumental Filters on Electrochemical Measurement of Single-Nanoparticle Collision Dynamics. *ChemElectroChem* **2018**, *5* (20), 3059−3067.
(24) Martín-Yerga, D.; Costa-García, A.; Unwin, P. R. Correlative Voltammetric Microscopy: Structure-Activity Relationships in the Microscopic Electrochemical Behavior of Screen Printed Carbon Electrodes. *ACS Sensors* **2019**, *4*, 2173−2180.
(25) Hutton, L.; Newton, M. E.; Unwin, P. R.; Macpherson, J. V. Amperometric Oxygen Sensor Based on a Platinum Nanoparticle-Modified Polycrystalline Boron Doped Diamond Disk Electrode. *Anal. Chem.* **2009**, *81* (3), 1023−1032.
(26) Gao, X.; Omosebi, A.; Landon, J.; Liu, K. Surface Charge Enhanced Carbon Electrodes for Stable and Efficient Capacitive Deionization Using Inverted Adsorption-Desorption Behavior. *Energy Environ. Sci.* **2015**, *8* (3), 897−909.
(27) Bath, B. D.; Michael, D. J.; Trafton, B. J.; Joseph, J. D.; Runnels, P. L.; Wightman, R. M. Subsecond Adsorption and Desorption of Dopamine at Carbon-Fiber Microelectrodes. *Anal. Chem.* **2000**, *72* (24), 5994−6002.
(28) Zeng, Y.; Prasetyo, L.; Nguyen, V. T.; Horikawa, T.; Do, D.; Nicholson, D. Characterization of Oxygen Functional Groups on Carbon Surfaces with Water and Methanol Adsorption. *Carbon* **2015**, *81*, 447−457.
(29) Desimoni, E.; Casella, G.; Morone, A.; Salvi, A. XPS Determination of Oxygen-containing Functional Groups on Carbon-fibre Surfaces and the Cleaning of These Surfaces. *Surf. Interface Anal.* **1990**, *15* (10), 627−634.
(30) Peltola, E.; Sainio, S.; Holt, K. B.; Palomäki, T.; Koskinen, J.; Laurila, T. Electrochemical Fouling of Dopamine and Recovery of Carbon Electrodes. *Anal. Chem.* **2018**, *90* (2), 1408−1416.
(31) Cao, Q.; Puthongkham, P.; Venton, B. J. Review: New Insights into Optimizing Chemical and 3D Surface Structures of Carbon Electrodes for Neurotransmitter Detection. *Anal. Methods* **2019**, *11* (3), 247−261.
(32) DuVall, S. H.; McCreery, R. L. Self-Catalysis by Catechols and Quinones during Heterogeneous Electron Transfer at Carbon Electrodes. *J. Am. Chem. Soc.* **2000**, *122* (28), 6759−6764.
(33) Patel, A. N.; Tan, S.; Miller, T. S.; Macpherson, J. V.; Unwin, P. R. Comparison and Reappraisal of Carbon Electrodes for the Voltammetric Detection of Dopamine. *Anal. Chem.* **2013**, *85* (24), 11755−11764.
(34) Amatore, C.; Arbault, S.; Bonifas, I.; Bouret, Y.; Erard, M.; Ewing, A. G.; Sombers, L. A. Correlation between Vesicle Quantal Size and Fusion Pore Release in Chromaffin Cell Exocytosis. *Biophys. J.* **2005**, *88* (6), 4411−4420.
(35) Meunier, A.; Bretou, M.; Darchen, F.; Guille Collignon, M.; Lemaître, F.; Amatore, C. Amperometric Detection of Vesicular Exocytosis from BON Cells at Carbon Fiber Microelectrodes. *Electrochim. Acta* **2014**, *126*, 74−80.

https://doi.org/10.1021/acsmeasuresciau.1c00006
ACS Meas. Au 2021, 1, 6−10